

Poster Abstracts

P1. 7071-A-2423

Recurrence of atrial fibrillation after new-onset transient episode during ST-elevation myocardial infarction

Marina Demidova^{1,2}, Maria Baturova^{1,3}, David Erlinge¹, Pyotr Platonov¹

¹ Department of Cardiology, Lund University, Sweden, ² Department of Cardiac Physiology, Institute of Physiology, Komi Science Center, Ural Branch, Russian Academy of Sciences, Syktyvkar, Russia, ³ North-West Center for diagnostics and treatment of arrhythmias, Saint-Petersburg, Russia

Background: Atrial fibrillation (AF) often complicates ST-elevation myocardial infarction (STEMI). The data on AF recurrence (re-AF) after new-onset AF during STEMI is scarce, and electrocardiographic (ECG) predictors of re-AF are unknown.

Purpose: Our aim was to assess the risk and to find out the predictors of re-AF after new-onset transient AF during STEMI.

Methods: STEMI patients discharged after primary PCI during 2007-2010 were followed until 2018. Clinical characteristics, date of AF diagnosis and mortality status were retrieved from the Swedish national registries. All ECGs recorded before, during or after STEMI were exported in digital format. New AF was defined as first-ever AF episode occurring between symptom onset and hospital discharge. P-wave indexes were assessed from the latest sinus rhythm ECG before discharge. The endpoint was the first documented AF episode after discharge. Patients with pre-existing AF and new AF discharged with AF were excluded from the endpoint analysis. Cox regression analysis was adjusted for age, gender and ejection fraction.

Results: Of the 2131 STEMI patients discharged alive, 164 (7.6%) had pre-existing AF, 138 (6.4%) had new-onset AF and 1,829 had no AF either before or during STEMI (NoAF). Patients from NewAF group were more likely to develop AF during follow-up (n=74 [58.3%]) than those from NoAF group (n=56 [3.1%], HR=4.80 95%CI 3.93-5.97) (Figure). None of the clinical and demographic characteristics was associated with re-AF. P-wave duration, P-terminal force in V₁ and P amplitude in lead I were associated with re-AF, however only reduced P-wave amplitude in lead I was independently associated with re-AF (P-amplitude <93 μ V HR=1.75 95%CI 1.03-2.99).

Conclusion: New-onset AF in STEMI is associated with increased risk of AF after discharge. ECG-based P-wave indexes reflecting atrial remodeling can be used for the prediction of re-AF after discharge.

Prediction of ablation index and lesion size index for local impedance drop-guided ablation in atrium

Lukas Sprenger, Vera Maslova, Adrian Zaman, Marc Nonnenmacher, Sven Willert, Derk Frank, Thomas Demming, Evgeny Lyan

Lukas Sprenger UKSH Campus Kiel, Germany

Background and Purpose: Local impedance (LI) drop dynamics predict lesion transmuralty. Furthermore, the LOCALIZE trial shows that a durable conduction block is achievable without calculating lesion indexes. As next-generation ablation catheters combine CF and LI monitoring, our study aims to compare an index-guided ablation (AI and LSI) to a sole LI-guided approach.

Methods: Today, next-generation ablation catheters combine CF and LI monitoring (Stablepoint, RHYTHMIA HDx™ with DIRECTSENSE™). While no lesion indexes are available on this platform and AI and LSI formulas contain proprietary coefficients, we chose a two-step approach.

1. Two custom machine learning models based on a Random Forest Regressor were trained on ablation data exported from their corresponding mapping systems. Yielding 529,684 and 42,538 data points, in cross-validation, both algorithms highly predicted their according indices, respectively (R2 0.972, MAE 6.62 and R2 0.973, MAE 0.07).

2. We retrospectively analysed atrial ablation data of 27 patients undergoing LI drop-guided ablation. Raw impedance data passed through a 1.5s moving mean filter, and the impedance minimum defined the LI drop point/plateau. We then performed AI and LSI calculations for every time point on the ablation trace. An AI of ≥ 400 and an LSI of ≥ 4 were set as target values.

Results: Table 1 shows the main results. 58% and 33% of all lesions reached the set target with shorter ablation duration in both indices target groups. However, only the AI group showed statistical significance. Most importantly, both target groups' initial and mean CF values are higher.

Conclusions: Solely LI-guided ablation results in increased ablation duration as compared to index-guided ablation. However, further clinical studies are necessary to identify the clinical impact of a shorter ablation duration on a reliable conduction block and the mitigation of complications.

Table 1: Ablation parameters of the lesions created

| | AI-target ≥ 400 matched | | LSI-target ≥ 4 matched | | No match group* |
|---|------------------------------|----------|-----------------------------|----------|--------------------------|
| | <i>Md (IQR)</i> | <i>p</i> | <i>Md (IQR)</i> | <i>p</i> | <i>Md (IQR)</i> |
| Number of lesions, n (%) | 191 (58) | - | 108 (33) | | 30 (9) |
| Time to LI drop plateau, s | 15.31 (12.06 - 25.57) | <.001 | 12.74 (9.67 - 18.26) | .006 | 7.56 (3.38 - 20.39) |
| Time to AI ≥ 400 , s | 6.16 (4.24 - 8.41) | .005 | 5.59 (4.0 - 7.81) | .001 | 8.27 (4.83 - 13.67) |
| Time to LSI ≥ 4 , s | 12.4 (5.86 - 31.12) | .338 | 6.68 (3.94 - 12.24) | .062 | 11.03 (5.48 - 31.11) |
| AI at LI drop plateau | 518.18 (473.97 - 551.95) | <.001 | 500.38 (435.0 - 547.71) | <.001 | 353.83 (313.75 - 377.47) |
| LSI at LI drop plateau | 3.96 (3.09 - 4.47) | <.001 | 4.51 (4.29 - 5.21) | <.001 | 2.97 (0.31 - 3.3) |
| Starting CF, g | 18.37 (11.29 - 26.22) | .001 | 17.76 (11.0 - 26.99) | .003 | 11.31 (7.46 - 18.85) |
| Mean CF, g | 18.98 (13.06 - 27.58) | .002 | 19.74 (12.69 - 29.24) | .002 | 11.39 (9.5 - 22.58) |
| LI drop, Ohm | 19.09 (15.12 - 24.44) | .018 | 18.12 (13.87 - 24.42) | .095 | 14.5 (10.27 - 21.01) |
| Starting LI, Ohm | 137.34 (125.89 - 145.24) | .545 | 132.83 (124.13 - 140.3) | .486 | 133.39 (125.62 - 143.87) |
| Closest distance to neighbouring lesion, mm | 4.05 (3.11 - 4.93) | .045 | 4.1 (3.21 - 5.14) | .041 | 3.21 (2.3 - 4.64) |

*Neither AI- nor LSI-target are matched

P3. 7101-A-2423

Mild cognitive dysfunction assessment in patients with atrial fibrillation utilizing the R4Alz assessment test

Maria Toumpourleka¹, Dimitrios Tachmatzidis¹, Magdalini Meletidou¹, Konstantinos Triantafyllou¹, Antonios Antoniadis¹, Georgios Giannopoulos¹, Vassilios Vassilikos¹

¹Third Cardiology Department, Aristotle University of Thessaloniki, Hippokraton Hospital, Thessaloniki, Greece

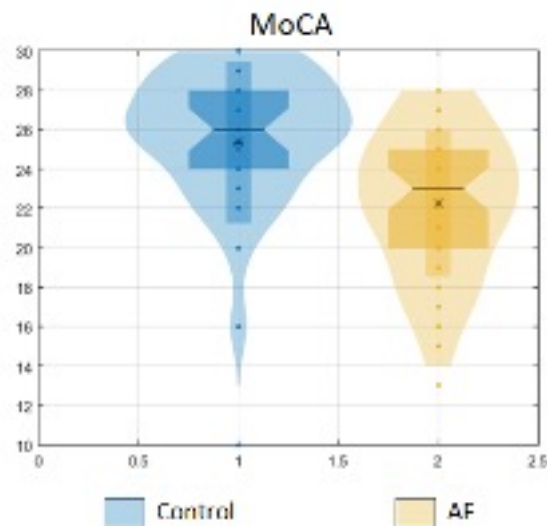
Background: Atrial fibrillation (AF) is associated with cognitive dysfunction, however, establishing such a diagnosis remains challenging, especially in oligosymptomatic patients. REMEDES for Alzheimer (R4Alz) is a novel test, designed to assess cognitive control decline at an early stage.

Purpose: We sought to evaluate the prevalence of early, mild cognitive dysfunction in patients with paroxysmal AF with the use of established and novel diagnostic tools.

Methods: This is a prospective cross-sectional study at a tertiary center that enrolled consecutive patients with paroxysmal AF and matched healthy controls. History of stroke or known cognitive dysfunction were exclusion criteria. Both groups were subjected to Montreal Cognitive Assessment (MoCA) and to R4Alz within the same day. R4Alz assesses cognitive function and attention ability at three stages: working memory updating (R1), supervisory attention system (R2) and task/rule switching and control of inhibition (R3). The primary endpoint was the difference in cognitive function between patients with AF and controls. Statistical analysis was performed with R version 4.1.0 and a p-value<0.05 was considered statistically significant.

Results: Fifty-five patients with AF and thirty-four controls were enrolled in the study (Mean age: 62.6 y, Female gender: 62.9%). MoCA scores (25.4 ± 4.11 for patients with AF vs 22.3 ± 3.72 for healthy controls, p-value <0.001) (Figure 1) as well as scores of all stages of R4ALz {working memory updating (R1a, R1b, R1c), supervisory attention system (R2) and task/rule switching – inhibition control (R3a1, R3a2, R3b)} were indicative of mild cognitive dysfunction in patients with AF. The control group exhibited significantly better cognitive performance on all assessment tools.

Conclusions: Assessment by established and novel tools revealed increased prevalence of mild cognitive impairment in patients with paroxysmal AF, compared to healthy matched controls



P4. 7073-A-2423

Brain natriuretic peptide levels are significantly elevated among patients with paroxysmal atrial fibrillation: insights from the PLACEBO study

Vassilios Vassilikos¹, Aristi Boulmpou¹, Anastasios Tsarouchas¹, Christodoulos Papadopoulos¹, Georgios Zormpas², Antonios Antoniadis¹, Aikaterini Vassilikou¹, Alexandros Evangeliou¹, Magdalini Petridou¹, Georgios Giannakoulas³

¹ Third Department of Cardiology ATh, Ippokratio General Hospital of Thessaloniki, Greece, ² Second Department of Cardiology ATh, Ippokratio General Hospital of Thessaloniki, Greece, ³ First Department of Cardiology ATh, AHEPA University Hospital, Thessaloniki, Greece

Background: BNP is elevated in cardiac conditions such as heart failure (HF) and atrial fibrillation (AF), and represents a useful tool for the diagnosis and evaluation of these disease states in clinical practice. Patients with permanent AF demonstrate elevated BNP values; it has been reported that BNP levels are elevated among patients with paroxysmal AF (PAF) around the arrhythmic episodes. BNP levels in patients with PAF free from events for a significant time period could highlight the risk for developing future AF episodes.

Purpose: We aimed to identify BNP levels of patients with PAF, without HF, measured at least 2 weeks following an AF episode.

Methods: We analyzed data from the Ergospirometry in Paroxysmal Atrial Fibrillation Prognosis (PLACEBO) trial (NCT05246423), an observational, prospective, single-center cohort study aiming to examine the prognostic role of CPET variables in future AF paroxysms. We included 54 patients with PAF and 30 healthy individuals. BNP was measured in all participants and at least 2 weeks after the last AF paroxysm.

Results: Our study cohort comprised 83 participants (54 patients with PAF and 30 controls). Baseline demographics are presented in the relevant table. Patients with PAF were older than controls and they had higher incidence of comorbidities, as expected. BNP levels, although within normal limits, were significantly higher among patients with PAF compared to healthy individuals [25(16) versus 63(91)pg/mL, p<0.001].

Conclusions: Our results demonstrate significantly increased BNP levels among patients with PAF compared to controls, assessed at least 2 weeks after the last AF episode. Our findings reflect a significant cardiac chamber overloading and inflammation that might be associated with the increased prevalence of comorbidities observed in the more "aged" group of PAF patients, even after a considerable free of events time period. When combined with a series of other variables, BNP may assist in the prediction of future AF episodes.

| Variable | Patients with PAF (n=54) | Controls (n=30) | p-value |
|------------------------------------|---------------------------------|------------------------|----------------|
| <i>Age (years)</i> | 60.4 (13.8) | 51 (26.6) | <0.001 |
| <i>Female sex (%)</i> | 46 | 51 | 0.080 |
| <i>BMI</i> | 27.8 (4.7) | 25.5 (4.7) | 0.031 |
| <i>Smoking (n)</i> | 18 | 11 | 0.758 |
| <i>Diabetes mellitus (n)</i> | 6 | 0 | 0.058 |
| <i>Hypertension (n)</i> | 25 | 3 | 0.001 |
| <i>Dyslipidemia (n)</i> | 28 | 7 | 0.011 |
| <i>Alcohol (n)</i> | 29 | 19 | 0.393 |
| <i>Exercise, any type (n)</i> | 38 | 22 | 0.773 |
| <i>Heart failure (n)</i> | 1 | 0 | 0.453 |
| <i>Coronary artery disease (n)</i> | 1 | 0 | 0.453 |
| <i>Thyroid disease (n)</i> | 10 | 3 | 0.301 |
| <i>Hemoglobin (mg/dL)</i> | 13.4±1.1 | 14±1.3 | 0.077 |
| <i>RDW (%)</i> | 13.6 (0.9) | 13.4 (0.9) | 0.019 |
| <i>Hs-cTnl (pg/mL)</i> | 2.7 (2.4) | 2.7 (2.5) | 0.900 |
| <i>BNP (pg/mL)</i> | 63 (91) | 25 (16) | <0.001 |

P5. 7282-A-2423

Derived vectorcardiographic analysis provides additional information for atrial fibrillation prediction in heart failure

Gary Tse¹, Jiandong Zhou², Beni Mehrdad Shahmohammadi¹, Rajesh Rajan³, Jeffrey Chan³, Guoliang Li⁴, George Bazoukis⁵, Guangping Li⁴, Kangyin Chen⁴, Tong Liu⁴

¹ Hong Kong Metropolitan University, ² University of Hong Kong, ³ Cardiovascular Analytics Group, Hong Kong, ⁴ Second Hospital of Tianjin Medical University, China, ⁵ Larnaca General Hospital, Cyprus

Background: Electrocardiographic (ECG) predictors of atrial fibrillation (AF) have often focused on P-wave abnormalities. However, vector-related information of not only P-waves but also of the QRS complex, ST segment and T-wave may provide additional value for AF risk stratification. This study evaluated the vectorcardiographic (VCG) information from derived ECG waveforms for predicting new onset AF in heart failure (HF).

Methods: This study included Chinese patients with HF between January 2010 and December 2016 from a single tertiary hospital. Cox regression was used to identify predictors (hazard ratios (HRs) and 95% confidence intervals). Angles were measured in degrees and areas were measured in Ashman units (40 ms x 0.1 mV).

Results: A total of 2506 patients were included (48.8% male, baseline age 77.1[66.7-84.1] years old). The initial angle of the QRS vector in the transverse plane (HR: 1.001 95% CI:[1.001-1.002]; P=0.0018), P-wave frontal axis (1.00[1.00-1.01];P<0.0001), P-wave horizontal axis (1.007[1.006-1.008];P<0.0001), QRS frontal axis (1.002[1.001-1.003];P<0.0001), ST segment frontal axis (1.003[1.003-1.004];P<0.0001) and horizontal axis (1.00[1.00-1.01];P<0.0001), T-wave frontal axis within the initial 40 ms (1.003[1.001-1.004];P<0.0001), T-wave frontal axis (1.001[1.001-1.002]; P=0.0007) and T-wave horizontal axis (1.001[1.001-1.002];P<0.0001) within the terminal 40 ms, and overall T-wave frontal axis (1.001[1.000-1.003]; P=0.0072) were significant predictors of AF, as were a lower mean T-wave area (0.91[0.90-0.93];P<0.0001) and higher T wave area (1.37 [1.12-1.67];0.0019).

Conclusions: T-wave areas from automated ECG analysis, reflecting the dispersion of the ventricular repolarization, as well as derived vectorcardiographic information on the directions of P-wave, QRS, ST and T-wave propagation, were predictive of AF.

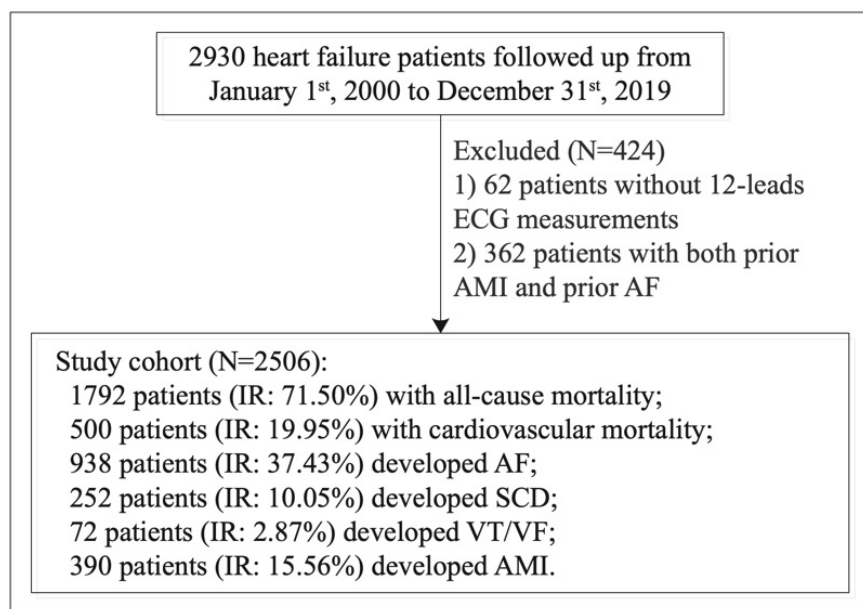


Figure 1. Procedures of data processing.

IR: incidence rate; VT/VF: ventricular tachycardia/ventricular fibrillation; AF: atrial fibrillation; AMI: acute myocardial infarction.

Investigating the effect of RR series characteristics on hemodynamics

Felix Plappert¹, Pim J. A. Oomen^{2,3}, Pyotr G. Platonov⁴, Mikael Wallman⁵, Frida Sandberg¹

¹ Department of Biomedical Engineering, Lund University, Lund, Sweden, ² Department of Biomedical Engineering, University of California, Irvine, Irvine, CA, USA, ³ Edwards Lifesciences Foundation Cardiovascular Innovation and Research Center, University of California, Irvine, Irvine, CA, USA, ⁴ Department of Cardiology, Clinical Sciences, Lund University, Lund, Sweden, ⁵ Department of Systems and Data Analysis, Fraunhofer- Chalmers Centre, Gothenburg, Sweden

Introduction: Currently, rate control in atrial fibrillation (AF) is purely based on heart rate with lenient heart rate <110 bpm as the recommended target. However, it remains unclear how sensitive the hemodynamics are to changes in RR series variability RRV and RR series irregularity RRI compared to changes in mean RR interval RRM.

Purpose: The purpose of this study is to assess the impact of RRV and RRI on cardiac output and left ventricular pressure and volume across a range of RRM.

Methods: We modeled changes in hemodynamics with a rapid electromechanical model of the heart and circulation. The atria and ventricles were modeled as spherical walls using the MultiPatch approach, where the onset of mechanical contraction of individual wall segments was controlled by electrical activation times. For the simulation study, a total of 9000 RR series of 200 beats were investigated, covering combinations of average heart rates between 70 and 150 bpm, low/high RRI, and low/high RRV (corresponding to sinus rhythm/AF).

Results: Figure 1 shows that increasing average heart rates result in a strict decrease in systolic pressure and diastolic volume and an increase-plateau-decrease trend in cardiac output. Compared to low RRV, high RRV result in a higher variation in systolic and diastolic pressure and volume in the left ventricle and a lower cardiac output. Changes in RRI result in minor effects on cardiac output for low heart rates.

Conclusions: Our simulation study indicates that changes in RRV have a large effect on distributions of systolic and diastolic pressure and volume, and the cardiac output. Since the cardiac output is similar at 110 bpm with high RRV and 120 bpm with low RRV the results indicate that not only RRM but also RRV are important measures for the hemodynamic impact of rate control.

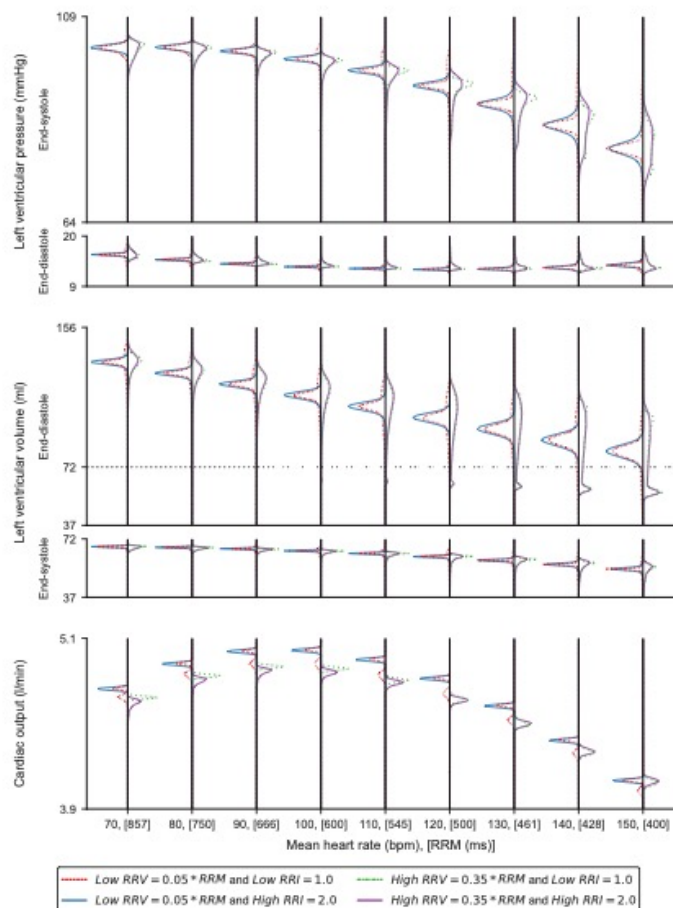


Figure 1. Systolic and diastolic pressures and volumes in the left ventricle, and cardiac output for a range of mean heart rates (or equivalently the mean RR interval RRM), RR series variabilities RRV and RR series irregularities RRI. For each heart rate, the distributions for low RRV are illustrated on the left side of the black vertical lines and high RRV are on the right side. The RRV is characterized by the root mean square of successive RR interval differences. Dotted lines represent low RRI and solid lines high RRI. The RRI is characterized by the sample entropy of the RR series. The samples in the distributions for systolic and diastolic pressure and volume are determined for each heart beat, while the samples in the distributions for the cardiac output are calculated for the whole RR series.

Prognostic value of synthesized right-side precordial leads in arrhythmogenic right ventricular cardiomyopathy: data from Nordic, Dutch, and Canadian ARVC registries

Aleksei Savelev¹, Daniel Guldenring², Anneli Svensson³, Pia Dahlberg⁴, Dewar Finlay⁵, Peter Doggart^{5,6}, Alan Kennedy⁶, Jesper H Svendsen⁷, Alex H Christensen⁸, Claus Graff⁹, Julia Cadrin-Tourigny¹⁰, Anneline S J M te Riele¹¹, Pyotr G Platonov¹

¹ Department of Cardiology, Clinical Sciences, Lund University, Lund, Sweden, ² Faculty of Electrical Engineering, Kempten University of Applied Sciences, Kempten, Germany, ³ Department of Cardiology, Linköping University Hospital, Linköping, Sweden and Department of Health, Medicine and Caring Sciences, Linköping University, Linköping, Sweden, ⁴ Department of Cardiology, Department of Molecular and Clinical Medicine, Institute of Medicine, Sahlgrenska Academy, Gothenburg, Sweden, ⁵ Ulster University, Belfast, UK, ⁶ PulseAI, Belfast, UK, ⁷ Department of Cardiology, the Heart Centre, Rigshospitalet, University of Copenhagen, and Department of Clinical Medicine, Faculty of Health and Medical Sciences, University of Copenhagen, Copenhagen, Denmark, ⁸ Department of Cardiology, Copenhagen University Hospital - Herlev-Gentofte, Herlev, Denmark and Department of Clinical Medicine, Faculty of Health and Medical Sciences, University of Copenhagen, Copenhagen, Denmark, ⁹ Department of Health Science and Technology, Aalborg University, Aalborg, Denmark, ¹⁰ Department of Medicine, Montreal Heart Institute, University of Montreal, Montreal, Canada, ¹¹ Division of Heart and Lungs, Department of Cardiology, University Medical Center Utrecht, Utrecht University, Utrecht, the Netherlands

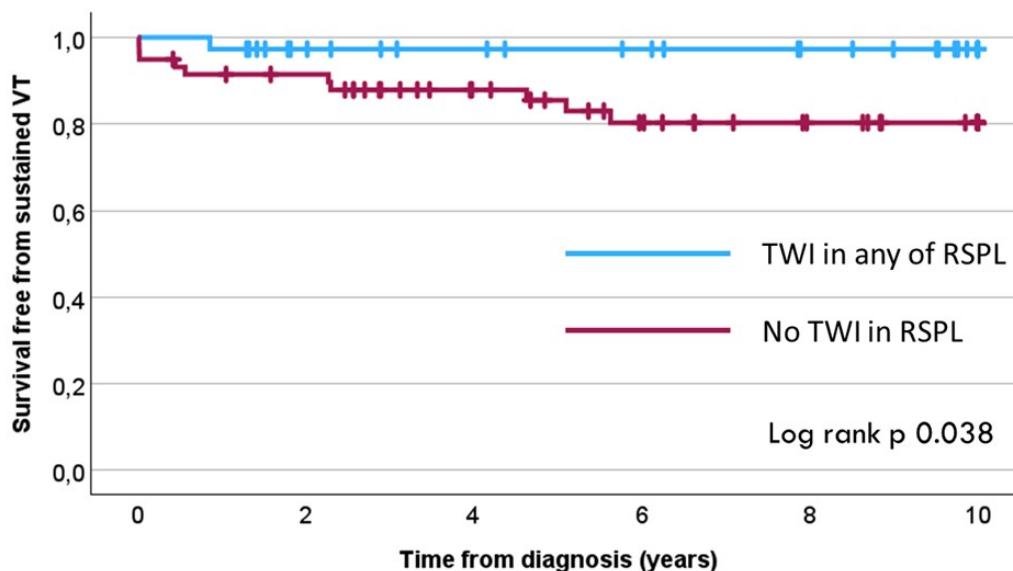
Background: T-wave inversion (TWI) in standard ECG leads is a proven risk marker for life-threatening ventricular arrhythmias (VA) in arrhythmogenic right ventricular cardiomyopathy (ARVC). Right-sided precordial leads (RSPL), which may be more sensitive for detection of the arrhythmogenic substrate, are understudied in this context.

Purpose: We aimed to assess the value of TWI in RSPL, synthesized from the standard 12-lead ECG, for prediction of VA risk in ARVC patients with subtle ECG phenotypes.

Methods: Patients with definite ARVC and no history of sustained VA prior to diagnosis from the Nordic, Canadian and Dutch ARVC registries were included. Patients with major repolarization criterion or complete right bundle branch block (RBBB) were excluded. RSPL (V3R-V6R) were derived from digitally recorded eight linearly independent leads (I, II and precordial V1 to V6) of the standard ECG using a linear ECG transformation matrix. TWI exceeding 0.1 mV in any of the synthesized leads was tested for its ability to predict sustained VA, defined as either sustained ventricular tachycardia, appropriate ICD shock, aborted cardiac arrest, or sudden cardiac death. Hazard ratio was calculated using Cox regression analysis adjusted for age, sex, and proband status.

Results: 96 patients comprised the study group (mean age 40±16, 42% female, 41% probands, 48% ICD-carriers). 59(62%) had TWI in one or more synthesized RSPL. During 10 years of follow-up, 11 patients (12%) developed VA. Kaplan-Meier curve analysis showed significant association between the presence of TWI in at least one of the RSPL and the risk of VA, which remained an independent predictor in the adjusted Cox regression analysis (HR 10.6, 95%CI 1.3-84.4, p=0.026).

Conclusions: Synthesized right-sided precordial leads appear to contain information potentially useful for refining risk stratification of primary prevention ARVC patients with a subtle ECG phenotype, in whom traditional repolarization markers are not informative.



Analysis of QT dispersion in an outpatient sotalol introduction safety protocol

Alberto Pereira Ferraz¹, Rodrigo Melo Kulchetscki¹, Tan Chen Wu¹, Luciana Sacilotto¹, Pedro Veronese¹, Marya Pagotti¹, Savia Bueno¹, Esteban Rivarolla¹, Denise Hachul¹, Maurício Scanavacca¹, Francisco Darrieux¹

¹Heart Institute (InCor), University of São Paulo Medical School

Background: Corrected QT dispersion (QTd) is accepted as a non-invasive method for detecting ventricular repolarization heterogeneity and electrical instability, being considered a marker of arrhythmogenesis.

Purpose: To describe the results of QTd in a safety outpatient based starting assessment of sotalol protocol.

Methods: Consecutive patients were initiated with oral sotalol in a tertiary center in Brazil according to approved labeled arrhythmias and inclusion criteria. Electrocardiographic analysis of heart rate (HR), corrected QT intervals (QTc) and QTd were performed by standard 12-lead electrocardiogram before sotalol bid administration, 2 hours after the first dose and after 3 days. The QTd was defined as the difference between the longest and shortest QTc measured on the 12-lead ECG.

Results: Fifty-five patients [median age 52,2 (21-86) years-old, 47% male, mean ejection fraction 60,8% ± 10,9] received an average dose of 73,1 ± 9,6 mg of sotalol per intake (bid). The median HR decreased before sotalol administration to the other evaluated moments [69 (55-95) bpm before sotalol, 62 (41-88) bpm 2h-after sotalol and 63 (42-94) bpm after-three-days, p<0.05], but no difference was found between the 2h-after and the after-three-days doses (p>0.999). Two patients presented QTc variation greater than 10% (13.5% and 12.0%), but none more than 15% or beyond 500ms. The median QTd was 38 (6-93) ms, 40,5 (4-91)ms and 38 (15-103)ms for the before-sotalol, 2h-after and after-3-days doses, respectively. There was no statistically significant difference of the QTd measurements between doses (p = 0.925).

Conclusion: There were no significant changes in QTd according to this protocol. These findings were conformable with no significant increase in QTc (increase less than 15% and interval not beyond 500ms). Larger studies are needed to assess the value of QTd in this population.

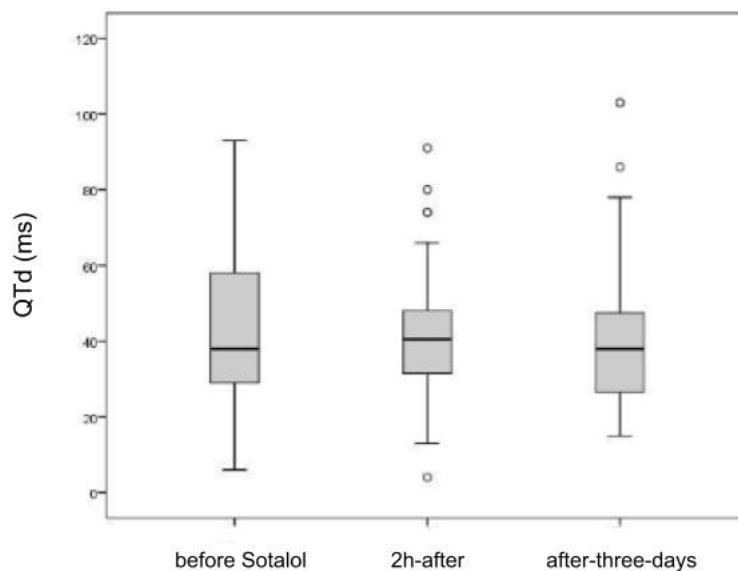


Figure 1 - Boxplot of QTd according to assessment moments

Endocardial and epicardial biventricular mapping of ventricular fibrillation

Elena Tolkacheva¹

¹ University of Minnesota, USA

Background: Ventricular fibrillation (VF) is a lethal cardiac arrhythmia that is a significant cause of sudden cardiac death. Comprehensive studies of spatiotemporal characteristics of VF in situ are difficult to perform with current mapping systems and catheter technology.

Objective: We aimed to develop a computational approach to characterize VF in a large animal model evaluating intracardiac electrograms during biventricular mapping of the endocardium (ENDO) and epicardium (EPI) in canine studies.

Methods: To develop thresholds for organized and disorganized activity, a Linear Discriminant Analysis (LDA)-based approach was performed to activities recorded in ex vivo Langendorff-perfused hearts using optical mapping experiments. Subsequently, VF was sequentially mapped in 4 canine hearts, using the CARTO mapping system with a multipolar mapping catheter in the ENDO left and right ventricles and EPI to capture the progression of VF at 3 discrete postinduction time intervals: VF period 1 (just after induction of VF to 15 minutes), VF period 2 (15 to 30 minutes), and VF period 3 (30 to 45 minutes). The developed LDA model, cycle lengths (CL), and regularity indices (RI) were applied to all recorded intracardiac electrograms to quantify the spatiotemporal organization of VF in canine hearts.

Results: We demonstrated the presence of organized activity in the EPI as VF progresses, in contrary to the ENDO, where the activity stays disorganized. The shortest CL always occurred in the ENDO, especially the RV, indicating faster VF activity. The highest RI was found in the EPI in all hearts for all VF stages, indicating spatiotemporal consistency of RR intervals.

Conclusion: We identified electrical organization and spatiotemporal differences throughout VF in canine hearts from induction to asystole. The RV ENDO is characterized by a high level of disorganization and faster VF frequency. In contrast, EPI has a high spatiotemporal organization of VF and consistently long RR intervals.

ECG-reflection of ventricular action potentials triangulation (simulation study)

Natalia Artyeva¹, Jan Azarov¹

¹ Laboratory of Cardiac Physiology, Institute of Physiology, Komi Science Center, Ural Branch, Russian Academy of Sciences, Russia

Background: Action potential (AP) triangulation due to disproportionate plateau shortening or phase 3 prolongation under drug administration is associated with arrhythmogenesis. The development of ECG-indices of AP triangulation requires the knowledge of AP morphology expression in the body surface ECG, which remains largely unclear thus far.

Purpose: to study in silico the ECG expression of AP morphology in conditions of disproportionate AP shortening/prolongation.

Methods: T-waves were simulated using a realistic rabbit model based on experimental data. The total action potential duration (APD), plateau phase duration and phase 3 duration were taken as APD at the level of 90% repolarization (APD₉₀), APD at the level of 30% repolarization (APD₃₀), and APD₉₀-APD₃₀, respectively. AP triangulation was simulated by the plateau shortening by 50% and by the phase 3 prolongation by 50 to 200%.

Results: AP triangulation due to the shortened plateau phase had no effect on T-wave morphology, amplitude and symmetry, while triangulation due to the prolonged phase 3 produced low-amplitude highly asymmetric T-waves, with the ascending limbs much longer than the descending limbs. In all simulations, the interval between the start (T_s) and the peak (T_p) of the T-wave (T_sT_p) divided by the interval between the J point and the start of the T-wave (JTs), a recently proposed ECG-index of AP triangulation, reflected (APD₉₀-APD₃₀)/APD₃₀ ratio. A tangent method for T_s instant detection provided the best approximation in all cases except the most flattened T-waves, when both the tangent and the baseline methods yielded similar results.

Conclusions: The simulations showed that AP triangulation was reflected in the body surface ECG differently depending on whether it was caused by the plateau phase shortening or the phase 3 prolongation. Regardless, the T_sT_p/JTs ratio corresponded well to the phase3/plateau ratio in all simulations

Experimental reproduction of diabetic ventricular arrhythmogenesis: mechanisms and manifestations

Alexey Ovechkin¹, Ekaterina Sedyakina¹, Alena Tsvetkova¹, Mikhail Gonotkov¹, Alexandra Durkina¹, Olesya Bernikova¹, Jan Azarov¹

¹ Institute of Physiology, Komi Science Center, Ural Branch of Russian Academy of Sciences, Russia

Background: Experimental data on arrhythmogenesis in diabetic animals are conflicting.

Purpose: The purpose of the study was to evaluate the effect of the duration of experimental diabetes mellitus (DM) on cardiac electrical remodeling and ventricular tachycardia and/or ventricular fibrillation (VT/VF) incidence.

Methods: Experiments were done in 23 control and 36 diabetic (streptozotocin model) male Wistar rats. The diabetic rats were divided into short and long DM groups (20 rats, 4-5 weeks and 16 rats, 8 weeks, respectively). Unipolar electrograms were recorded from 64 epicardial leads along with body surface ECG. Myocardial ischemia was induced by 5-min left anterior descending coronary artery ligation followed by reperfusion. Patch-clamp studies were performed in the cardiomyocytes isolated from the hearts after the in vivo experiments.

Results: QT and Tpeak-Tend intervals were prolonged in ECGs in the diabetic animals. Baseline (preischemic) dispersion of repolarization was significantly greater in the short DM group as compared to the controls. The reperfusion VT/VF incidences in the control, short DM, and long DM groups were 39.1% (9 of 23), 50.0% (8 of 16), and 6.3% (1 of 16), respectively ($p=0.015$, for short DM vs long DM). In the whole-cell patch-clamp experiments, action potential duration was prolonged in the diabetic animals, I_{Na} current was increased in the rats with short DM and decreased in the rats with long DM, the I_{CaL} current was increased in both diabetic groups, the I_{to} current was preserved in the short DM group and decreased in the long DM group.

Conclusions: Short-term (1 month) DM was associated with the increased duration and dispersion of repolarization manifesting in the increased QT and Tpeak-Tend intervals, resulting in the highest arrhythmogenicity and caused by the increased depolarizing and preserved repolarizing ionic currents.

Initial results of Mahaim pathway study in pediatric patients: case series

Frances Celine Melendres¹, Daniel Lee Cortez²

¹ University of California, Berkeley, ² Division of Pediatric Cardiology, Department of Pediatrics, University of California Davis Medical Center

Background: Mahaim accessory pathways are characterized by long, anterograde, decremental conduction with variable proximal and distal insertions. This study aims to add to the existing literature on Mahaim pathways specifically within the pediatric population.

Methods: A retrospective chart review was performed of patients with palpitations and pre-excitation who underwent EP study and ablation between August 2021 and December 2023 at the UC Davis Medical Center. Identification of patients found to have a Mahaim pathway was performed and EKG/perioperative details were reviewed.

Results: Seven patients with Mahaim pathways were identified with the median age being 12 years (range 5- 19 years) with 71% male patients. The presenting symptoms were palpitations and dizziness in all patients with one patient having related syncope. All patients had QRS notching noted with a left bundle branch morphology in V1 with late transition. Dual atrioventricular nodal physiology was present in 86% of patients. The Median cycle length of Mahaim tachycardia was 280 milliseconds (ms) with location on the tricuspid annulus from a left anterior oblique position being 8 to 12 o'clock. During tachycardia, all patients had a long post-pacing interval minus tachycardia cycle length (>115ms) and short Stim-Atrial minus ventricular to atrial interval of <85ms. Additional accessory pathways were noted in 71% of patients.

Conclusion: Mahaim tachycardia can present in young patients with a high abundance of additional accessory pathways noted. QRS notching in a pre-excited EKG with left bundle branch morphology may be of help in identifying a patient with possible Mahaim pathway conduction. PPI- TCL>115ms and SA minus VA<85ms may give a clue to Mahaim tachycardia in the setting of an antidromic SVT.

Internal jugular vein approach for complex congenital ablation: a case report

Frances Celine Melendres¹, Daniel Lee Cortez²

¹ University of California, Berkeley, ² Division of Pediatric Cardiology, Department of Pediatrics, University of California Davis Medical Center

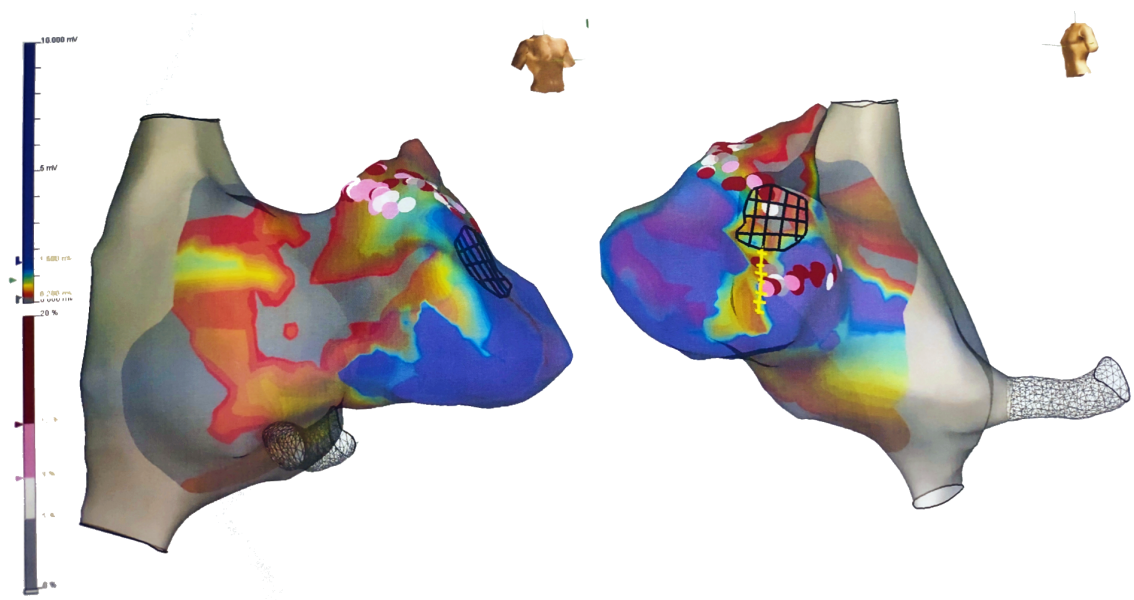
Background: Congenital heart disease (CHD) is associated with early surgical correction and late-onset complications such as cardiac arrhythmias. In the case of a complex CHD, ablative treatment of arrhythmias can be limited by catheter access which is generally performed through the femoral vein, which is sometimes not available as an access route in some patients.

Methods: A dialysis-dependent patient with repaired Tetralogy of Fallot, and sickle cell disease presented to our hospital after VT/VF arrest requiring defibrillation at an outside hospital. He was started on amiodarone but given his age of 33 years, referred to our institution. We demonstrated the feasibility of ablation of complex arrhythmias from a superior access (right internal jugular vein) using the EnSite/NavX system and the HD grid and bidirectional 3.5-millimeter irrigated TactiCath mapping and ablation catheters.

Results: Initial mapping of scar-based isthmus locations demonstrated intermittent high voltage points between the pulmonary valve and tricuspid valve isthmus as well as near the ventricular septal patch. Subsequent VT (poorly perfused VT) was demonstrated from the pulmonary valve to tricuspid valve isthmus and two from near the ventricular septal defect patch. These were ablated as well as cavotricuspid valve isthmus flutter and posterior right atrial ectopic atrial tachycardia.

Conclusion: Access can limit how to ablate patients, particularly in the setting of congenital heart disease and prior surgeries, thus alternative access routes, such as the internal jugular vein, can facilitate complex congenital ablations.

Figure 1. Map of Ventricular Tachycardia



Intracardiac left ventricular pressure-volume loops for pacemaker optimization in pediatric patients with complete heart block

Daniel Cortez¹, Guru Hiremath²

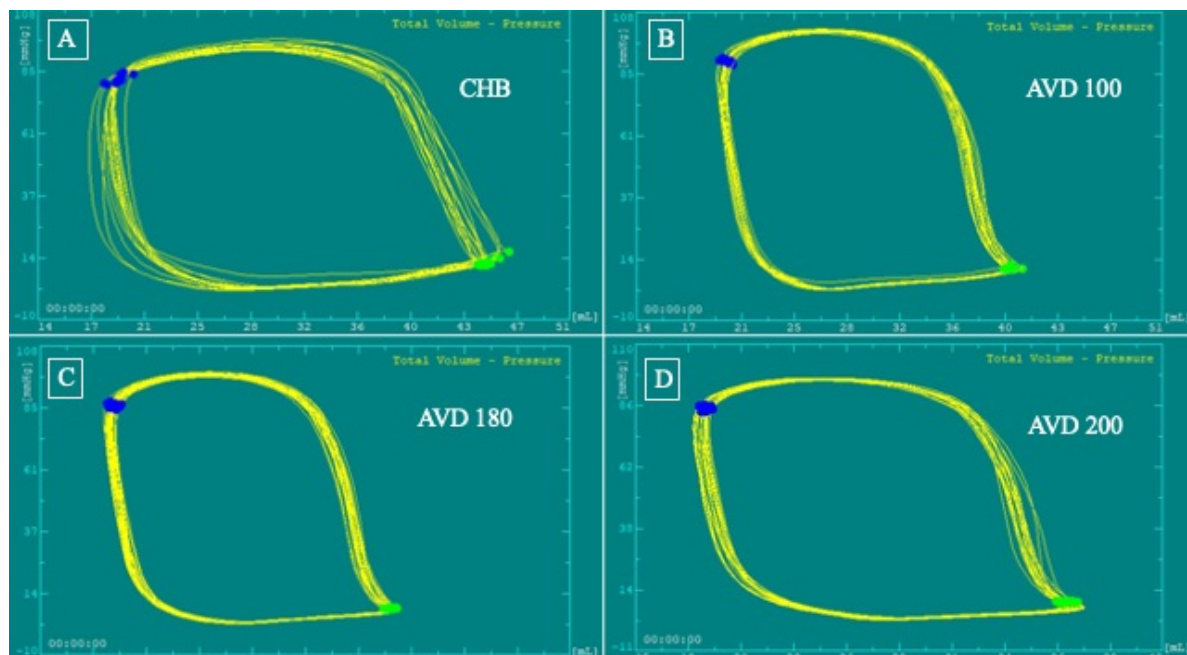
¹ UC Davis Medical Center, USA, ² University of Minnesota, USA

Introduction: Long-term pacing in the pediatric population requires a thoughtful consideration regarding type of pacing and its consequences. Long-term right ventricular pacing is associated with left ventricular dysfunction and cardiomyopathy in up to 13% or more of pediatric patients. There is no data about the use of intracardiac PV loops for pacemaker optimization in children. We decided to use intracardiac PV loops to help optimize pacemaker settings in children with complete heart block who underwent His-bundle pacing.

Methods: This is a single center retrospective case series of children under 18 years of age who underwent intracardiac PV loops to guide pacemaker optimization during placement of transvenous conduction system pacing for complete heart block between July 2018 and April 30th, 2020. Arterial access was obtained using a 7 fr sheath during the pacemaker implant procedure. After implantation of the transvenous pacemaker, a 7-Fr high-fidelity conductance catheter made by CD Leycom® (Hengelo, The Netherlands) was advanced into the left. The conductance catheters are connected to the Inca® PV Loop System to obtain real time PV loops (Figure 1). Pressure and volume calibration using hypertonic saline injected through a right heart catheter was performed as per published methods. Real time PV loops were obtained in baseline condition of complete heart block and during pacing with different AV delay intervals.

Results: Five patients were included in the study, with median age 11 years, with 80% female patients, and all patients having congenital complete heart block. The most improvement in stroke-work was at an AV delay of 130 and 180 milliseconds (ms) for all patients and change in pressure over time (dP/dt) was most improved at 180ms (Figure 2).

Conclusion: For a small cohort of adolescent patients undergoing conduction-system pacing, an atrioventricular delay of 180 milliseconds is associated with best stroke work change and dP/dt.



Comparative analysis of deep learning and conventional machine learning for heart arrhythmias/ECG pattern classification using optimal ECG lead sets.

Shijie Zhou¹, Serhii Reznichenko¹, John Whitaker², Zixuan Ni³

¹ Miami University, Oxford, 45056 OH, USA, ² St Thomas' Hospital, London UK, ³ Zhejiang University, Hangzhou, China

Background: Artificial Intelligence, particularly Deep Learning (DL), is evolving ECG interpretation with enhanced speed and accuracy. However, the comparative effectiveness of DL and Conventional Machine Learning (CML) remains unexplored, especially considering DL's need for larger datasets and CML's potential accuracy advantages in certain scenarios.

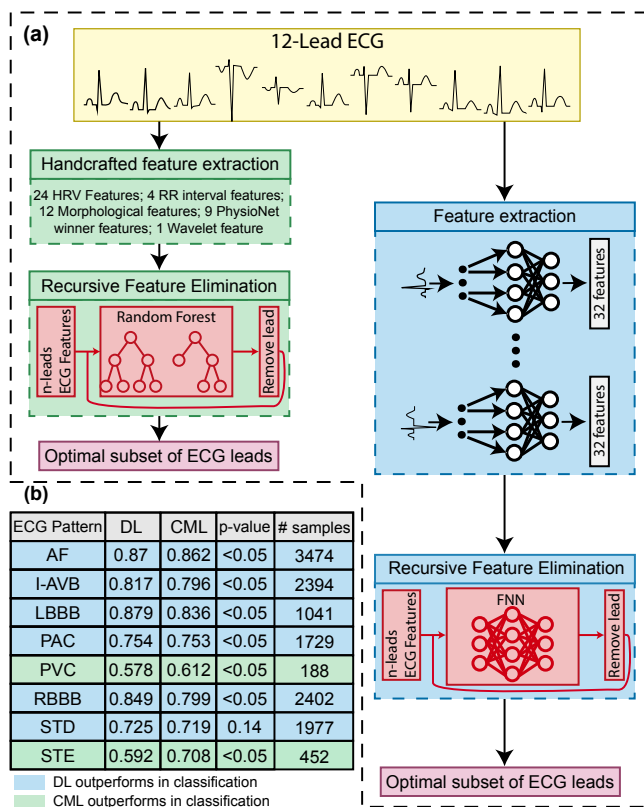
Objectives: To explore an optimal ECG-lead set for each arrhythmia/ECG pattern using DL and CML approaches, then to compare the classification performance of both DL and CML using the optimal ECG-lead subset.

Methods: We utilized the PhysioNet Cardiology Challenge 2020 dataset that consists of 8 arrhythmias/ECG patterns (STD, STE, I-AVB, PAC, PVC, LBBB, RBBB, AF), employing a Convolutional Neural Network classifier for DL and a Random Forest classifier for CML (Fig.1a). Both approaches used recursive feature elimination to identify optimal ECG-lead subsets (CML: Random Forest feature importance scores; DL: SHAP values). The optimal subset was determined based on statistical significance (p-value < 0.05) and F1-score.

Results: The CML required 72% more ECG leads than DL to identify an optimal ECG-leads subset in classifying each arrhythmia/ECG pattern, averaging 9 leads compared to DL's 5. Two common leads (I, II) were identified as optimal for the CML across 8 arrhythmias/ECG patterns, while no specific leads were consistently present in all the optimal subsets of ECG leads when using DL. The DL significantly outperformed the CML in classifying 5 arrhythmias/ECG patterns as shown in Fig. 1b. However, the DL was less effective for PVC and STE due to significantly fewer samples, suggesting CML's utility in cases with limited data.

Conclusion: The DL generally offers higher accuracy and a more generalized solution for ECG interpretation with fewer leads. However, for arrhythmias with limited data, CML may be more applicable, highlighting the importance of choosing the appropriate method based on the available dataset.

Figure 1. (a) The workflow depicting the approach of finding optimal subsets of ECG leads using the DL and the CML approaches. (b) The macro F1-scores for the DL and CML approaches for classification arrhythmias/ECG patterns using their optimal subsets of ECG leads.



P16. 7090-A-2423

As far as the eye can see: a new method of ECG filtering

Richard Redina^{1,2}, Marina Filipenska², Zdenek Starek¹

¹ International Clinical Research Center, Brno, Czech Republic, ² Brno University of Technology, Faculty of Electrical Engineering and Communication, Department of Biomedical Engineering, Brno, Czech Republic

Background/Introduction: Acquisition of a quality signal is an important prerequisite for proper follow-up diagnostics. The presence of various types of noise, which are not easily separable from the signal, often stands in the way of obtaining quality patient data.

Purpose: The main objective of our work was to implement a novel ECG filtering technique using artificial intelligence methods and unsupervised learning procedure.

Methods: A Blind-Spot convolutional neural network (BSN) was created for ECG filtering. This unsupervised learning method is suitable in the context of a priori unknown denoised signal, which is required when using supervised techniques. Two hyperparameters were optimized in order to obtain the best results: a) the size of the input kernel - the size of the segment entering the network – determining the network's ability to approximate an unknown signal element; b) the network's architecture. The BSN was trained and tested using ECGs degraded with artificial noise of level 2 to 15 dB. Data from a total of 100 patients with various arrhythmias were used.

Results: A series of experiments were performed on the available ECGs to test the model's ability to remove different types as well as different levels of noise. Signal-to-noise ratio (SNR) calculated for the denoised ECGs reached up to 12 dB. Root mean square error (RMSE) reached around 0.09 on normalized signals.

Conclusion: We present a novel method for filtering ECG recordings that is based on artificial intelligence while using an unsupervised learning approach. Given the very promising results, we anticipate that it could be a valuable contribution to classical methods using digital signal processing.

Validation of a machine learning based classification algorithm for ambulatory heart rhythm diagnostics using smartphone-photoplethysmography – the SMARTBEATS algorithm study

Jonatan Fernstad^{1,2}, Emma Svennberg³, Peter Åberg¹, Katrin Kemp Gudmundsdottir¹, Johan Engdahl^{1,2}

¹ Karolinska Institutet, Department of Clinical Sciences, Danderyd University Hospital, Stockholm, Sweden, ² Department of Cardiology, Danderyd University Hospital, Stockholm, Sweden, ³ Karolinska Institutet, Department of Medicine, Huddinge, Karolinska University Hospital, Stockholm, Sweden

Introduction: Smartphone-photoplethysmography (PPG) can be used for heart rhythm monitoring. According to current guidelines, ECG verification is required for a new diagnosis of atrial fibrillation (AF).

Purpose: The aim of this study was to validate an automatic algorithm for heart rhythm diagnostics using smartphone-PPG in patients with AF in an unsupervised ambulatory setting.

Methods: Patients undergoing direct current cardioversion (DCCV) at a university hospital for treatment of AF or AFL were asked to perform one-minute heart rhythm recordings post-treatment at least twice daily for 30 days at home. All participants were provided with an iPhone 7 smartphone running the CORAI Heart Monitor PPG application simultaneously with a single-lead ECG recording (KardiaMobile). ECG recordings were interpreted independently by two cardiologists and were set as gold standard. The CORAI-AF automatic algorithm uses support vector machines (SVM) to classify the heart rhythm from the smartphone-PPG recordings, and diagnostic performance was calculated with Leave-One-Subject-Out cross validation ensuring complete independence between training and test sets.

Results: In total 280 patients, median age 69.0 years (31% women), registered 18,005 simultaneous PPG and ECG recordings. Recordings interpreted as AFL on ECG (2.0%), as having insufficient quality on ECG (4.9%) or PPG (2.8%), and low certainty algorithmic classifications (1.5%) were excluded. Included ECG recordings consisted of 71.5% interpreted as sinus rhythm (SR) and 28.5% as AF. Algorithm classification of the PPG recordings diagnosed AF (sensitivity) in 99.7% and SR (specificity) in 99.8% of the recordings, with an overall accuracy of 99.8%. F1-score was 99.6% and area under the ROC curve (AUC) was 0.999.

Conclusion: A machine learning based algorithm for automatic heart rhythm diagnostics showed excellent diagnostic performance for smartphone-PPG recordings in an unsupervised ambulatory setting.

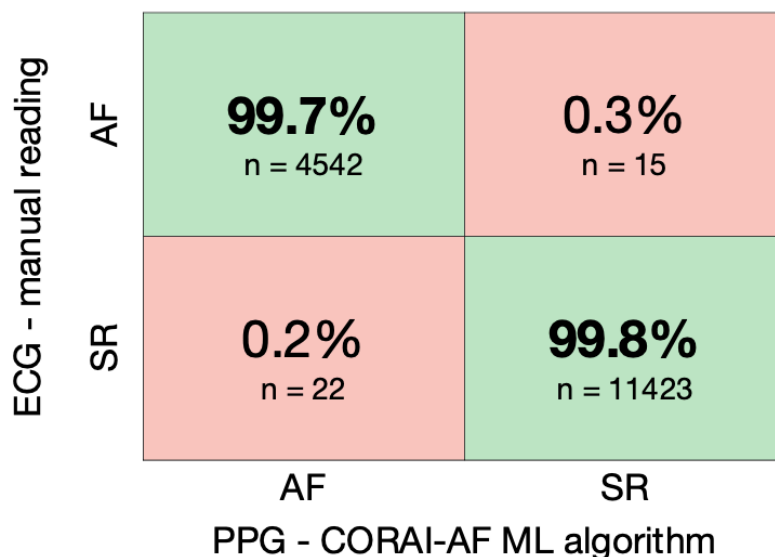


Figure 1. Diagnostic performance of a machine learning based automatic algorithm classifying heart rhythm from ambulatory smartphone-PPG recordings compared to manual reading of simultaneously recorded single-lead ECG: sensitivity: 99.7%, specificity: 99.8%, overall accuracy: 99.8%.

PPG: photoplethysmogram **ECG:** electrocardiogram **SR:** sinus rhythm **AF:** atrial fibrillation **ML:** machine learning

Enhancing 12-lead ECG reconstruction with comprehensive component parts as input

Ekenedirichukwu Obianom¹, André Ng¹, Xin Li¹

¹ University of Leicester, UK

Background: Previous research has aimed at identifying optimal subsets of leads for accurate lead reconstruction for full standard 12-lead electrocardiogram (ECG). Currently, I, II, and V2 are predominate in these reconstructions. Recent studies have shown that incorporating additional leads or features could enhance model performance.

Purpose: The primary aim of this work is to enhance ECG reconstruction performance by 1) evaluating the efficacy of leads V2 and V3 in the reconstructing 12-lead ECG, while also 2) proposing a new method incorporating ECG component parts (P wave, QRS complex, T wave) as inputs in the reconstruction process.

Method: 30s ECGs of a group of 80 patients (40 healthy and 40 with myocardial infarction), in PTB-Database, was used for this study. Component parts (as in figure 1b) are extracted from the ECG. Various linear regression models were built using the least square method. The different groups of inputs used are (A) I, II, V2 (B) I, II, V3 (C) I, II, V3 and component parts. The R-squared, correlation coefficient (r), and root-mean-square-error (RMSE) are calculated between the original signals and the model-reconstructed signals to compare the performance of models built for both generic models and patient specific models. Subject-wise five-fold cross validation was performed on each model.

Results: For the generic models, the average R-squared, r, RMSE for input-A are 0.659 ± 0.559, 0.910 ± 0.121, 0.086 ± 0.046mV respectively; input-B are 0.715 ± 0.385, 0.919 ± 0.111, 0.082 ± 0.046mV respectively; and input-C (ECGW) are 0.722 ± 0.391, 0.924 ± 0.112, 0.079 ± 0.047mV respectively. ECGW performed best with the highest average R-squared and r, and the lowest RMSE.

Conclusions: V3 should be used as a predictor in place of V2. The model incorporating components parts improved performance of models without increasing the number of leads needed for reconstruction.

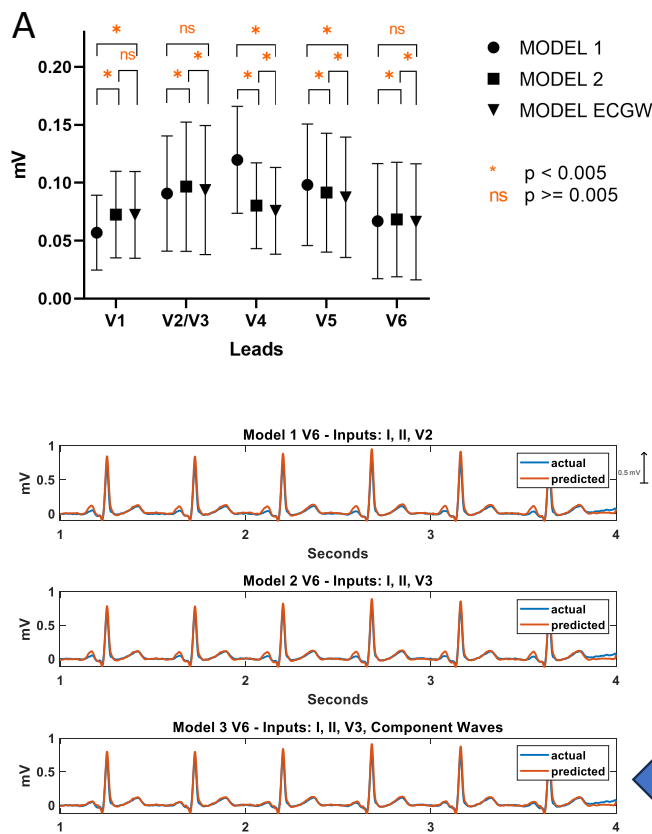
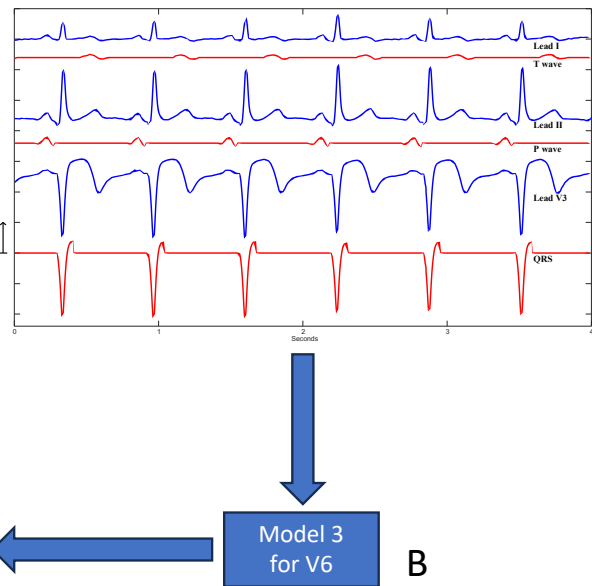


Figure 1: A) On the left, the graph of the RMSE, showing the p values between each model. B) Below, the flow diagram of the ECGW model with the results compared to other models.



Genome-wide association study of the electrocardiographic ST-segment reveals elevated risk of cardiac arrest

Rasmus Frosted^{1,2}, Oliver Bundgaard Vad^{3,4}, Laia Meseguer Monfort^{3,4}, Henning Bundgaard^{1,5}, Claus Graff⁶, Jørgen Kim Kanters^{7,8}, Morten Salling Olesen^{3,4}, Alex Hørby Christensen^{1,2,5}

¹ Department of Cardiology, The Heart Centre, Copenhagen University Hospital—Rigshospitalet, Copenhagen, Denmark, ² Department of Cardiology, Copenhagen University Hospital—Herlev-Gentofte Hospital, Herlev, Denmark, ³ Laboratory for Molecular Cardiology, Department of Cardiology, The Heart Centre, Copenhagen University Hospital—Rigshospitalet, Copenhagen, Denmark, ⁴ Department of Biomedical Sciences, Faculty of Health and Medical Sciences, University of Copenhagen, Copenhagen, Denmark, ⁵ Department of Clinical Medicine, Faculty of Health and Medical Sciences, University of Copenhagen, Copenhagen, Denmark, ⁶ Department of Health Science and Technology, Aalborg University, Aalborg, Denmark, ⁷ Laboratory of Experimental Cardiology, Department of Biomedical Sciences, University of Copenhagen, Copenhagen, Denmark, ⁸ Center of Physiological Research, University of California San Francisco, San Francisco, CA, USA.

Background: The ST-segment in electrocardiography represents the interval between ventricular depolarization and repolarization and is linked to conditions such as myocardial infarction, Brugada Syndrome, and early repolarization syndrome. Genome-wide association studies (GWAS) have been instrumental in unraveling the genetic basis of cardiovascular diseases. Despite this, there is a gap in understanding the genetic underpinnings of the ST-segment and its predictive value for clinical events.

Purpose: This study aimed to comprehensively investigate the genetic determinants of the ST-segment through a large-scale GWAS, investigate the underlying biological pathways, and evaluate the predictive power of a polygenic risk score (PRS).

Methods: We conducted a GWAS meta-analysis on ST-segment amplitude using data from two distinct cohorts: The Copenhagen Hospital Biobank and the UK Biobank (total n=109,168). Involved biological pathways were investigated incorporating 1000 Genomes Phase 3 data for LD reference. A PRS was generated and applied to an independent sample (n= 423,655). Additionally, we employed linkage disequilibrium score regression (LDSC) to assess correlations between ST-segment genes and associated cardiac traits or diseases.

Results: We discovered 94 loci (66 novel). Novel genes included NACA, CDKN1A, and SSBP3, whereas the pathway analysis revealed associations to, among others, heart development, cardiac contraction, regulation of membrane potential and the cation channel complex. The PRS applied to the independent sample showed a step-wise elevated risk for atrial fibrillation, ischemic heart disease, cardiac arrest, and heart failure associated with ST-segment deviation. The LDSC analyses unveiled associations with the PR-Interval and QTc, without associating with QRS, while showing an association with Brugada Syndrome.

Conclusion: Our discoveries contribute to a better understanding of the genetic basis of ST-segment deviations, uncovering previously unknown loci and genes. The established polygenic risk score shows promise in predicting important clinical outcomes including cardiac arrest, adding valuable insights to the field of cardiovascular genetics and precision medicine.

Sudden cardiac death may be caused by cardiac alpha-synuclein deposition

Keivan Javanshiri¹, Mattias Haglund¹, Elisabet Englund¹

¹ Division of Pathology, Department of Clinical Sciences, Lund University, Sweden

Objectives: The hallmark pathology in Lewy body disease (LBD) is alpha-synuclein (α -synuclein) aggregates. These aggregates have recently been reported to exist in the epicardial nerves in all stages of the disease, including preclinical stages. Their effects on the cardiac nerves and cardiac function are however unknown. The aim of this project was to investigate the cause of death as well as the prevalence of cardiovascular disease in a neuropathologically confirmed cohort with LBD.

Method: The immediate cause of death from autopsy reports was evaluated in 78 neuropathologically confirmed cases of LBD (brainstem, limbic or cortical). All cases had a histopathologically confirmed manifestation of cardiac α -synuclein. Autopsy cardiovascular data (i.e. severity of atherosclerosis in the coronary arteries, cardiac hypertrophy, myocardial infarction) as well as clinical data on cardio- and cerebrovascular disease (i.e. arrhythmias, congestive heart failure, elongated QTc, stroke), and risk factors (hypertension and diabetes mellitus type II) were also assessed. An age-matched group of 53 subjects with other major neurocognitive disease served as controls.

Results: The incidence of autopsy findings consistent with sudden cardiac death was 51.3% in the LBD group compared to 22.6% in the control group ($p < 0.001$). These cases had signs of terminal cardiac dysfunction without attributes of ischemic heart disease. No other differences were identified between the groups regarding other autopsy-reported cardiac findings and clinical cardio- and cerebrovascular disease, or risk factors. QTc interval did not differ significantly between cases of suspected SCD and other causes of death.

Conclusions: Sudden cardiac death may be an under recognized cause of death in LBD. Further research is needed to explore potential alterations in cardiac function caused by α -synuclein aggregates. LBD is often accompanied by autonomic dysfunction and falls due to orthostatic hypotension, which may mask clinically important arrhythmia.

Holter-based QT dispersion was useful to predict mortality within 6 months in patient with Covid-19 pneumonia.

Kenichi Hashimoto¹, Motohiro Kimata¹, Naomi Harada¹, Yusuke Kawamura¹, Yuji Kasamaki^{2, 1}
National Defense Medical College, ² Kanazawa Medical College Himi Municipal Hospital

Introduction: QT abnormalities in patients with COVID-19 pneumonia are known to be closely associated with severe cardiovascular events or mortality. Although QT dispersion is an indicator of QT abnormalities, there are few reports on QT dispersion (QTd) using high-resolution Holter electrocardiography (H-QTd).

Purpose: In the present study, we investigated the usefulness of H-QTd in patients with COVID-19 pneumonia.

Methods: The H-QTd of sixty-two COVID-19 patients (mean age 62.8 years, 37 males) were analyzed. The endpoints were all-cause mortality and fatal arrhythmia within 60 days of admission. QTd was measured for 15 seconds every hour, and dispersion was defined as the maximum QT difference between orthogonal X, Y, and Z leads. The mean QTd was defined as the average of the QTd measured for 15 seconds every hour. Heart rate variability (HRV) was also analyzed.

Results: Of the 62 patients, 10 patients died with the onset of COVID-19 pneumonia within 60 days. The mean H-QTd was significantly higher in the death group than in the survival group; 41.0 ms [29.0 ms, 72.4 ms] vs 85.3 ms [47.5 ms, 85.3 ms] (P= 0.006). In univariate logistic analysis,

HR [95% CI] = 0.391 [0.001-0.009], p= 0.013 for a mean H-QTd, and in multivariate analysis including left ventricular ejection fraction and HRV, mean H-QTd was an independent risk factor for all-cause mortality and fatal arrhythmia (HR [95% CI] =0.398 [0.001-0.007], p = 0.005). The cut-off value for H-QTd in the healthy group was 73 ms, calculated from the 95th percentile, and the sensitivity, specificity, positive predictive value and negative predictive value of the endpoint in COVID-19 patients were 50%, 93%, 56%, and 91.2%, respectively.

Conclusion: The mean H-QTd was suggested to be a potential prognostic indicator for patients with COVID-19 pneumonia.

Screening for postural orthostatic tachycardia syndrome using 24-hour ECG recording in patients with long COVID

David Hupin^{1,2}, Vincent Pichot², Magnus Bäck^{1,3}, Malin Nygren-Bonnier⁴, Ulrika Reistam^{1,3}, Michael Runold¹, Judith Bruchfeldt¹, Caroline Dupré², Antoine Da Costa⁵, Cécile Romeyer⁵, Frédéric Roche², Jean-Claude Barthelemy², Marcus Ståhlberg^{1,3}, Artur Fedorowski^{1,3,6}, Jannike Nickander⁷

¹Department of Medicine, Karolinska Institutet, Stockholm, Sweden; ²Univ Jean Monnet, Department of Clinical and Exercise Physiology, University Hospital of Saint-Etienne, Mines Saint-Étienne, INSERM, U 1059, Saint-Étienne, France; ³Department of Cardiology, Karolinska University Hospital, Stockholm, Sweden; ⁴Department of Neurobiology, Care Sciences and Society, Karolinska Institutet, Stockholm, Sweden; ⁵Univ Jean Monnet, Department of Cardiology, University Hospital of Saint-Etienne, Mines Saint-Étienne, INSERM, U 1059, Saint-Étienne, France; ⁶Department of Clinical Sciences, Lund University, Malmö, Sweden; ⁷Department of Molecular Medicine and Surgery, Karolinska Institutet, Stockholm, Sweden

Background: Cardiovascular autonomic dysfunction (CVAD) is a major complication in a large proportion of long COVID patients. One of the most typical phenotypes of CVAD, postural orthostatic tachycardia syndrome (POTS), is commonly observed as a sequelae of COVID infection, thus defining a subset of long COVID patients. Application of 24h-ECG recording in this patient group has not been explored.

Purpose: The objective of the study was to develop, test and validate 24h-ECG recording as a relevant diagnostic tool for POTS.

Methods: Consecutive patients referred to the multidisciplinary long COVID unit at Karolinska University Hospital in Stockholm, Sweden from April 2021 to April 2022 were included. Patients with POTS were compared with long COVID patients without POTS (verified by active standing test/head-up tilt testing) and control healthy subjects according to 3 specific analyses based on 24-h ECG recording: (1) heart rate (HR) spikes >30 bpm; (2) awakening HR increase; and (3) HR variability parameters. Control group consisted of healthy subjects from database of the University Hospital of Saint-Etienne, France.

Results: A total of 100 long-COVID patients (mean age: 42.54±10.45y, 92% women) and 100 healthy subjects (mean age: 41.40±7.21y, 96% women) were included. Long-COVID POTS (n=45) was associated with (1) higher number of HR spikes/h (1.47±0.84 vs. 0.40±0.28/h, p<0.01), (2) abrupt and sustained increase in HR after awakening (p<0.05), and (3) reduction of HRV (mean SDNN: 90.61±23.73 vs. 97.33±29.90 ms, p=0.04; mean RMSSD: 34.90±12.48 vs. 43.35±21.10 ms, p=0.04) compared with healthy subjects.

Conclusions: A triple analysis of 24-h ECG recordings could reveal a characteristic POTS signature in long COVID patients. This novel analysis may be introduced in the clinic for screening and therapy monitoring.

Thoracic impedance during national holidays

Anneli Olsson¹, Rebecca Rylance¹, Rasmus Borgqvist¹, David Erlinge¹, Pyotr Platonov¹

¹ Department of Cardiology, Lund University, Sweden

Background: Increased incidence of myocardial infarctions during Christmas and national holidays could possibly be caused by overindulgence in food and alcohol. Monitoring of decreased thoracic impedance (TI) by cardiac implantable electronic devices (CIED) has been a tool for detection of fluid accumulation. We aimed to assess the relationship between TI and national holidays in patients treated with CIED.

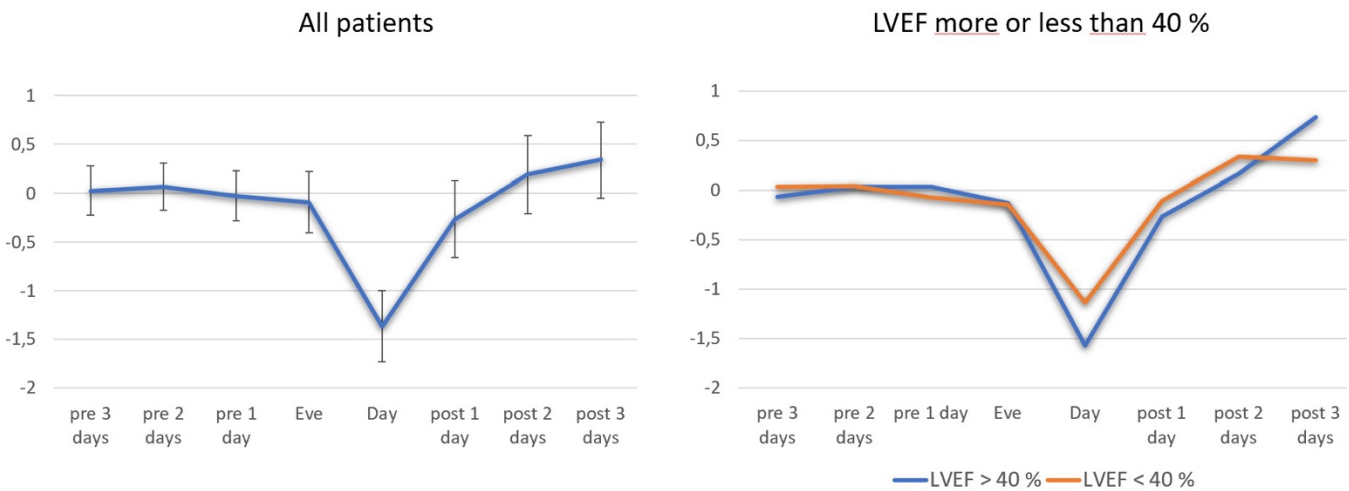
Method: Consecutive patients with CIED capable of TI monitoring enrolled in the remote monitoring program at a tertiary care hospital in Sweden were screened. A full disclosure remote CIED monitoring database containing daily measurements of TI and device therapy delivery provided the data source for this retrospective cohort study. Patients were included if they had data for at least one holiday (Christmas, New Year or Midsummer) between June 2015 and January 2020. TI during the holiday was compared with baseline values, defined as a mean value of three days preceding Christmas and Midsummer. Clinical characteristics were obtained from medical records.

Result: In total, 96 patients (82 % men, age 69±10 years, 92 % ICD, 78 % CRT, 72 % with LVEF<40%) were included, which provided data for 645 patient- holidays. TI decreased by a mean of 1.3 Ohm (95% CI -1.9 to -0.6, p< 0.001) on Christmas Day, 0.6 Ohm (95 % CI -1.4 to 0.1, p = 0.08) on New Years Day and 1.3 Ohm (95 %CI -2,0 to -0.6, p≤0.001) on Midsummer Day. These TI changes were not related to age, sex or LVEF greater than or less than 40%. One ventricular tachycardia event requiring shock therapy was documented.

Conclusion: A statistically significant transient decrease in thoracic impedance was evident during Christmas Day and Midsummer Day in CIED treated patients. It is possible that a decrease in thoracic impedance may contribute to the increased incidence of myocardial infarction during holidays

Impedance changes during holidays

- percent changes from baseline (mean, 95 % CI), 645 obs



Perfused rat heart model for studies of Takotsubo syndrome and its protective effects.

AmirAli nejat¹, Ermir Zulfaj¹, Yalda Kakaei¹, Ahmed Elmahdy¹, mana kalani¹, Abhishek Jha¹, abdulhussain hamiid¹, Björn Redfors¹, Elmir Omerovic¹

¹ University of Gothenburg, Sahlgrenska Hospital, Gothenburg, Sweden

Background: Takotsubo syndrome (TS) is a clinically significant form of acute heart failure characterized by transient apical akinesia and basal hypercontractility. Nevertheless, the insufficient understanding of the underlying pathophysiological mechanisms of TS persists. To bridge this knowledge gap, we created an in vivo TS-like rat model, garnering international acclaim. The objective of this research is to construct an ex vivo TS-like model employing isolated perfused rat hearts (Langendorff method). This approach allows for meticulous exploration of TS pathophysiology and assessment of its protective capabilities against ventricular fibrillation.

Methods: Sixteen Sprague-Dawley rats were divided into four groups: Control, 24-hour post-in-vivo TS induction, ex-vivo TS induction, and ex-vivo re-stressed hearts. TS was induced using isoprenaline and confirmed with echocardiography. Hearts were rapidly mounted onto a Langendorff apparatus within 75 seconds. Viability was assessed based on predefined criteria. Perfusion pressure, myocardial flow, temperature, pH, pO₂, pCO₂, left ventricular (LV) pressure, LV contractility (dp/dt), RPP, LVDP, and ECG were continuously monitored for 90 minutes.

Results: Echocardiography confirmed a TS-like phenotype in the beating hearts, characterized by apical akinesia and basal hypercontractility. Compared to control hearts, TS induction and isoprenaline stress led to significant increases in heart rate, RPP, LVDP, and dp/dt (p<0.05); (Fig. 1 A-D). Apical segments of TS hearts exhibited reduced action potential duration (p<0.05). based on the arrhythmia score and the ECG finding, there is a lower incidence of ventricular arrhythmias compared to controls (p<0.001); (Fig 1 E-F). Ex vivo echocardiographic findings and parameters aligned with the in vivo model, and perfused TS hearts showed comparable viability and stability to controls (Fig.2).

Conclusion: We successfully established an ex vivo TS-like model using isolated perfused rat hearts, following the Langendorff method. This model is a valuable tool for detailed studies on TS pathophysiology, contributing to a better understanding of this clinically significant syn

